Statistics of spectra for critical quantum chaos in one-dimensional quasiperiodic systems

Yoshihiro Takada,[1] Kazusumi Ino,[1] and Masanori Yamanaka[2]
[1]*Department of Pure and Applied Sciences, University of Tokyo, Komaba 3-8-1, Meguro-ku, Tokyo, 153-8902, Japan*
[2]*Department of Physics, College of Science and Technology, Nihon University, Kanda-Surugadai 1-8, Chiyoda-ku, Tokyo, 101-8308, Japan*

(Received 26 December 2003; revised manuscript received 30 July 2004; published 3 December 2004)

We study spectral statistics of one-dimensional quasiperiodic systems at the metal-insulator transition. Several types of spectral statistics are observed at the critical points, lines, and region. On the critical lines, we find the bandwidth distribution $P_B(w)$ around the origin (in the tail) to have the form of $P_B(w) \sim w^{\alpha}[P_B(w) \sim e^{-\beta w^{\gamma}}]$ $(\alpha, \beta, \gamma > 0)$, while in the critical region $P_B(w) \sim w^{-\alpha'}$ $(\alpha' > 0)$. We also find the level spacing distribution to follow an inverse power law $P_G(s) \sim s^{-\delta}$ $(\delta > 0)$.

DOI: 10.1103/PhysRevE.70.066203 PACS number(s): 05.45.Mt, 71.30.+h, 03.65.Sq, 71.23.An

I. INTRODUCTION

The universality of statistical properties of the energy spectrum is ubiquitously found in quantum physics [1], ranging from quantum chaos [2] to quantum chromodynamics [3]. In condensed matter physics, the metal-insulator (MI) transition in disordered electron systems gives a notable example of such universality. On the metallic side, the energy level statistics can be described by random matrix theory [4,5]. The level spacing distribution is close to the Wigner surmise. The universality class is classified by the symmetry of the system. On the insulating side the level spacing distribution is Poissonian. At the critical point, different statistical features emerge [6,7]. They are different from random matrix theory and Poisson statistics. The universality of these statistics dubbed "critical level statistics" is also classified by the symmetry of the ensemble [8–13].

Quasiperiodic systems are other interesting ones showing the MI transition. The universality of the transition has been characterized by multifractal structures of bandwidths and wave functions (see Ref. [14] for a review). The Harper model [15–17] is obtained by gauge fixing of two-dimensional electrons on the square lattice in a uniform magnetic field. In particular, the incommensurate limits of the flux per plaquette, such as the inverse of the golden mean $\sigma = (-1+\sqrt{5})/2$, have been extensively studied. On the atomic scale, the penetration of flux for each plaquette requires an enormous strength of magnetic field, but nowadays it is realized in the laboratory on a quantum dot lattice [18].

The quasiperiodic system can be seen as a system between "periodic" and "random," thus giving an interesting example of quantum "chaos." Classically an open orbit (separatrix) of equienergetic curves appears at the MI transition point. But the quantum transition cannot be understood by classical considerations. It is not characterized by a single energy band corresponding to the separatrix but the wave functions for all the energy bands become critical with power-law decay. The energy level statistics are different from those of disordered systems. It is not close to the Wigner surmise on the metallic side nor is it the Poisson statistics seen on the insulating side [19]. Spectra of quasiperiodic systems have a fractal structure [15,16], which hinders established techniques used in the disordered case such as "unfolding" from extracting universal properties of fluctuations.

Recently, Evangelou and Pichard [20] investigated the bandwidth distribution $P_B(w)$ (w is the bandwidth) of the one-dimensional Harper model at the incommensurate limit of σ. They found that it agrees with the semi-Poisson statistics $P_B(w) = 4we^{-2w}$ with the sub-Poisson number variance $\Sigma_2(E) \sim \text{const} + \chi E$ $(\chi < 1)$ at the critical point. They argued that it is related to the universal characterization of quantum chaos.

Although this suggests that a characterization by level statistics is possible for the MI transitions of a larger class of quasiperiodic systems, the universal appearance of the semi-Poisson statistics may be questioned from the experience in critical level statistics of disordered systems. In Ref. [8], it has been suggested that the level spacing distribution may be described by a more generalized form $P(s) = As^{\alpha}e^{-\beta s^{\gamma}}$ $(\alpha, \beta, \gamma > 0)$. Although this simple form is not valid, the power-law behavior at the origin and the exponential decay in the tail (with $\gamma = 1$) have been observed in numerical studies and classified according to the symmetry of the system [9–13]. A similar rich structure of critical level statistics should be expected for quasiperiodic systems.

Motivated by this idea, we investigate a generalization of the Harper model, namely, the extended Harper model, which is obtained from two-dimensional electrons on the square lattice with next-nearest-neighbor hopping in a uniform magnetic field [21,22]. We find that such a rich structure indeed emerges for the critical level statistics of this

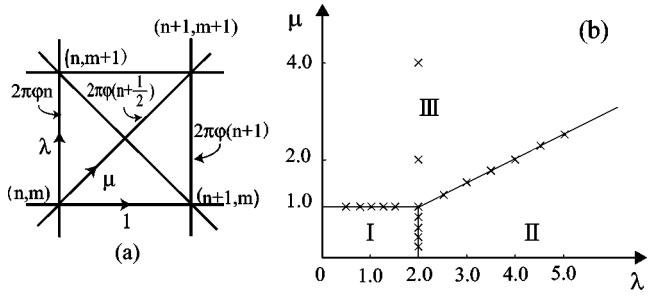

FIG. 1. (a) Transfer integrals and phases of the extended Harper model [Eq. (9)] and (b) its phase diagram (see [21]). In region I the wave function (spectrum) is extended (absolutely continuous) and in region II it is localized (pure points). In region III and on the three boundary lines, it is critical (singular continuous).

extended model, but with some substantial modifications, even for the case treated in [20]. We explain this variety of critical level statistics by the quantum nature of the system. The extended Harper model is considered as a single parameter deformation of the Harper model and contains the Harper model as a special value of the parameter. The MI transition point in the Harper model continues to a critical line with the introduction of the deformation parameter and the line extends to a critical area with increase in the parameter. Therefore, the extended model has the unique property of perturbing the universal behavior at the MI transition point.

II. MODEL

A. Harper model

The Harper model [23] is derived as a model for a two-dimensional electron in a magnetic field and a periodic potential. The Hamiltonian can be written in the form

$$H = t_x \cos x + t_y \cos p_x \tag{1}$$

where

$$p_x = -2\pi i \varphi \frac{d}{dx} \tag{2}$$

is the variable conjugate to the coordinate x. The corresponding model defined in a two-dimensional lattice is written as

$$H = t_x \sum_{n,m} c^{\dagger}_{n+1,m} e^{\theta_{n+1,m;n,m}} c_{n,m} + t_y \sum_{n,m} c^{\dagger}_{n,m+1} e^{\theta_{n,m+1;n,m}} c_{n,m} + \mathrm{H.c.} \tag{3}$$

where $c_{n,m}$ is the annihilation operator of a lattice fermion at a site (n,m) and $\Sigma_{plaquette}\theta_{\vec{r}}=2\pi\varphi$ is the magnetic flux around a plaquette. Here we assume a uniform flux. We take the Landau gauge, i.e., $\theta_{n+1,m;n,m}=0$ and $\theta_{n,m+1;n,m}=2\pi\varphi n$.

Let $|\Psi\rangle$ be a single-particle state,

$$|\Psi\rangle = \sum_{n,m} \Psi(n,m) c^{\dagger}_{n,m} |0\rangle. \tag{4}$$

By acting H on $|\Psi\rangle$, we obtain the Schrödinger equation

$$t_x[\Psi(n+1,m) + \Psi(n-1,m)] + t_y[e^{-2\pi i\varphi n}\Psi(n,m+1) + e^{2\pi i\varphi n}\Psi(n,m-1)] = E\Psi(n,m). \tag{5}$$

We consider anisotropy in hopping and set the transfer integral in the x direction as 1, and that in the y direction as λ. Since Eq. (5) is translationally invariant in the y direction, we may write $\Psi(n,m)=e^{-i\nu m}\psi_n$ and we obtain

$$\psi_{n+1} + \lambda \cos(2\pi n\varphi + \nu)\psi_n + \psi_{n-1} = E\psi_n. \tag{6}$$

This describes a one-dimensional quasiperiodic system when φ is irrational. It is known [17] that if $0<\lambda<2$, all the eigenstates are extended and if $2<\lambda$, all the eigenstates are localized. At the transition point $\lambda=2$ the spectrum is singular continuous; moreover, the states are neither localized nor extended. The phase diagram is shown in the $\mu=0$ line of Fig. 1(b).

B. Extended Harper model

The continuum version of the extended Harper model is

$$H = t_x \cos x + t_y \cos p_x + t_{xy}\cos(p_x - x) + t_{yx}\cos(p_x + x). \tag{7}$$

The lattice version of the model is obtained with introduction of next-nearest-neighbor hopping to the model (3). The Hamiltonian is

$$H = t_x \sum_{n,m} c^{\dagger}_{n+1,m} e^{\theta_{n+1,m;n,m}} c_{n,m} + t_y \sum_{n,m} c^{\dagger}_{n,m+1} e^{\theta_{n,m+1;n,m}} c_{n,m} + t_{xy} \sum_{n,m} c^{\dagger}_{n+1,m+1} e^{\theta_{n+1,m+1;n,m}} c_{n,m} + t_{yx} \sum_{n,m} c^{\dagger}_{n,m+1} e^{\theta_{n,m+1;n+1,m}} c_{n+1,m} + \mathrm{H.c.} \tag{8}$$

We set nearest-neighbor hopping for the perpendicular direction as λ, and next-nearest-neighbor hopping as μ, where nearest-neighbor hopping for the horizontal direction is set to be unity. The corresponding single-electron Schrödinger equation is

$$\left\{1 + \mu \cos\left[2\pi\left(n+\frac{1}{2}\right)\varphi + \nu\right]\right\}\psi_{n+1} + \lambda \cos(2\pi n\varphi + \nu)\psi_n + \left\{1 + \mu \cos\left[2\pi\left(n-\frac{1}{2}\right)\varphi + \nu\right]\right\}\psi_{n-1} = E\psi_n. \tag{9}$$

At $\mu=0$, this is reduced to the Harper model. The phase diagram is shown in Fig. 1(b). The scaling property of the bandwidths was studied in [21].

III. NUMERICAL ANALYSIS

A. Method

To investigate the incommensurate limit of $\varphi\to\sigma$, we use the rational approximation of $\varphi_j=p/q$ where p and q are relatively prime. We also set $\nu=0$ for simplicity. We will use the Fibonacci sequence $\varphi_j=F_{j-1}/F_j$, where F_j is the Fibonacci number satisfying $F_{j+1}=F_j+F_{j-1}$ with $F_0=1$ and $F_1=1$. For rational φ_j Eq. (9) reduces to a $q\times q$ matrix with the boundary condition $\psi_{n+q}=\exp(ikq)\psi_n$, which is

$$H = \begin{pmatrix} \lambda_1 & \mu_1 & 0 & \cdots & & & 0 & e^{ikq}\mu_0 \\ \mu_1 & \lambda_2 & \mu_2 & 0 & \cdots & & & 0 \\ 0 & \mu_2 & \lambda_3 & \mu_3 & 0 & \cdots & & 0 \\ & 0 & \mu_3 & \lambda_4 & \mu_4 & 0 & \cdots & 0 \\ \vdots & \vdots & \ddots & \ddots & \ddots & \ddots & \ddots & \vdots \\ 0 & & \cdots & 0 & \mu_{q-3} & \lambda_{q-2} & \mu_{q-2} & 0 \\ 0 & & & \cdots & 0 & \mu_{q-2} & \lambda_{q-1} & \mu_{q-1} \\ e^{-ikq}\mu_q & 0 & & & \cdots & 0 & \mu_{q-1} & \lambda_q \end{pmatrix}, \tag{10}$$

where $\lambda_n=\lambda\cos(2\pi n\varphi)$, $\mu_n=1+\mu\cos[2\pi(n+1/2)\varphi]$, and the basis is $(\psi_1,\psi_2,\ldots,\psi_n)$.

The k dependence of the energy bands E is obtained from

the consideration of the characteristic polynomial of Eq. (10). According to Ref. [22], the k dependence arises only from the constant term independent of E. The term is proportional to $\cos qk$ for fixed ν. The extreme of E is determined by the extreme of the constant term. Then the minimum and maximum of each energy band are obtained at either $k=0$ or π/q. Thus to obtain the bandwidths, we only need to consider these two values.

If the matrix size q is an odd integer, the matrix can be transformed to be tridiagonal by a simple base change [22]. The first transformation is just a rearrangement of the order of the base and H is transformed to

$$H' = \begin{pmatrix} \lambda_s & \mu_{s-1} & 0 & \cdots & \cdots & \cdots & \cdots & \cdots & 0 & \mu_s \\ \mu_{s-1} & \lambda_{s-1} & \mu_{s-2} & 0 & \cdots & & & & \cdots & 0 \\ 0 & \ddots & \ddots & \ddots & \ddots & & & & & \vdots \\ \vdots & \ddots & \mu_2 & \lambda_2 & \mu_1 & 0 & \cdots & & & \vdots \\ 0 & \cdots & 0 & \mu_1 & \lambda_1 & e^{ikq}\mu_0 & 0 & \cdots & & 0 \\ 0 & & \cdots & 0 & e^{-ikq}\mu_q & \lambda_q & \mu_{q-1} & 0 & \cdots & 0 \\ 0 & & & \cdots & 0 & \mu_{q-1} & \lambda_{q-1} & \mu_{q-2} & 0 & 0 \\ \vdots & & & & & \ddots & \ddots & \ddots & \ddots & \vdots \\ 0 & \cdots & & & & \cdots & 0 & \mu_{s+2} & \lambda_{s+2} & \mu_{s+1} \\ \mu_s & 0 & \cdots & \cdots & \cdots & \cdots & \cdots & 0 & \mu_{s+1} & \lambda_{s+1} \end{pmatrix}, \tag{11}$$

where $s=(q-1)/2$. We have used the following properties. (i) Since $\varphi_n=p/q=F_{n-1}/F_n$, the value of $\lambda_q=\lambda\cos(2\pi q\varphi_n)$ is always equal to λ. (ii) $\lambda_j=\lambda\cos(2\pi jp/q)=\lambda\cos[2\pi(-j)p/q+2\pi p]=\lambda\cos[2\pi(q-j)p/q]=\lambda_{q-j}$. (iii) In the same way, $\mu_j=\mu_{q-j-1}$.

We need the eigenvalues of matrix (10) for $k=0$ and $k=\pi/q$. For these values, H' becomes a real symmetric matrix and can be transformed to a tridiagonal matrix H^{trd} as follows:

$$H^{trd} = P^{-1}H'P \tag{12}$$

where

$$P = \begin{pmatrix} \frac{1}{\sqrt{2}} & 0 & 0 & \cdots & 0 & \cdots & 0 & 0 & \frac{1}{\sqrt{2}} \\ 0 & \frac{1}{\sqrt{2}} & 0 & \cdots & 0 & \cdots & 0 & \frac{1}{\sqrt{2}} & 0 \\ 0 & 0 & \ddots & \ddots & \vdots & \iddots & \iddots & 0 & 0 \\ \vdots & \vdots & \ddots & \frac{1}{\sqrt{2}} & 0 & \frac{1}{\sqrt{2}} & \iddots & \vdots & \vdots \\ \vdots & \vdots & \cdots & 0 & 1 & 0 & \cdots & \vdots & \vdots \\ \vdots & \vdots & 0 & \frac{1}{\sqrt{2}} & 0 & -\frac{1}{\sqrt{2}} & 0 & \vdots & \vdots \\ \vdots & \iddots & \iddots & 0 & \vdots & 0 & \ddots & \ddots & \vdots \\ 0 & \frac{1}{\sqrt{2}} & \iddots & \vdots & \vdots & \vdots & \ddots & -\frac{1}{\sqrt{2}} & 0 \\ \frac{1}{\sqrt{2}} & 0 & \cdots & \cdots & 0 & \cdots & \cdots & 0 & -\frac{1}{\sqrt{2}} \end{pmatrix} \tag{13}$$

and $P^{-1}=P^t=P$. Finally we can get the tridiagonal Hamiltonian

$$H^{trd} = \begin{pmatrix} a_1 & b_1 & 0 & \cdots & 0 & 0 & 0 \\ b_1 & a_2 & b_2 & \ddots & \ddots & 0 & 0 \\ 0 & b_2 & a_3 & \ddots & \ddots & \ddots & 0 \\ \vdots & \ddots & \ddots & \ddots & \ddots & \ddots & \vdots \\ 0 & \ddots & \ddots & \ddots & a_{q-2} & b_{q-2} & 0 \\ 0 & 0 & \cdots & \cdots & b_{q-2} & a_{q-1} & b_{q-1} \\ 0 & 0 & 0 & \cdots & 0 & b_{q-1} & a_q \end{pmatrix} \tag{14}$$

where the diagonal elements a_n $(n=1,2,\ldots,q)$ are

$$\begin{aligned} \{a_n\} &= (a_1,a_2,\ldots,a_{q-1},a_q) \\ &= (\lambda_s+\mu_s,\lambda_{s-1},\lambda_{s-2},\ldots, \\ &\quad \lambda_2,\lambda_1,\lambda_q,\lambda_{q-1},\ldots,\lambda_{s+3},\lambda_{s+2},\lambda_{s+1}-\mu_s) \end{aligned}$$

and the off-diagonal elements b_n $(n=1,2,\ldots,q-1)$ are

$$\begin{aligned} \{b_n\} &= (b_1,b_2,\ldots,b_{q-2},b_{q-1}) \\ &= \left(\mu_{s-1},\mu_{s-2},\ldots,\mu_1,\frac{1}{\sqrt{2}}(e^{ikq}\mu_0+\mu_{q-1}),\right. \\ &\quad \left.\frac{1}{\sqrt{2}}(e^{-ikq}\mu_0-\mu_{q-1}),\mu_{q-2},\mu_{q-3},\ldots,\mu_{s+1}\right). \end{aligned}$$

We numerically diagonalize the $q\times q$ matrices (14) and calculate the band edge. We obtain the bandwidth distribution $P_B(w)$ by subtraction of them. The normalizations are

$$\int_0^\infty P_B(w)dw = 1, \quad \langle w\rangle = \int_0^\infty wP_B(w)dw = 1. \tag{15}$$

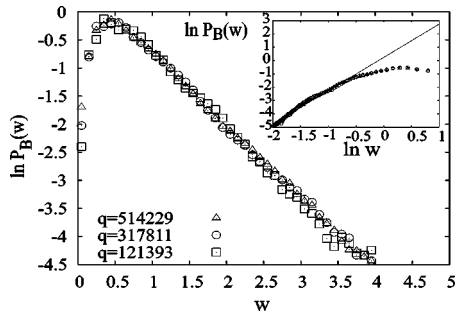

FIG. 2. The bandwidth distribution at $(\lambda,\mu)=(2.0,0.4)$, and the one near the origin (inset) for several q.

Similary, the gap distribution $P_G(s)$ is obtained and the normalizations are

$$\int_0^\infty P_G(s)ds = 1, \quad \langle s\rangle = \int_0^\infty sP_G(s)ds = 1. \tag{16}$$

B. Bandwidth distribution on $\lambda=2$

First, we study the bandwidth distribution along the critical line $\lambda=2$. In Fig. 2, we plot the $P_B(w)$ at $(\lambda,\mu)=(2.0,0.4)$ for $j=25$, 27, 28 where j is the index of F_j. It shows a good convergence to a limiting distribution, indicating the existence of the limit of the bandwidth distribution at the incommensurate flux φ. For $0\leqslant\mu<1$, we find that $P_B(w)$ exhibits a continuous change. It has been concluded [21] that the scaling property of the bandwidths is invariant on this line, implying that the system belongs to the same universality class. The continuous change means that $P_B(w)$ is not a universal quantity.

In Fig. 2, one sees linear behaviors at large w, implying an asymptotic form

$$P_B(w) \sim e^{-\beta w} \text{ as } w\to\infty \tag{17}$$

where $\beta>0$. The optimized values of β are shown in Table I. It suggests a quadratic dependence of β on μ. The best fit is attained by a quadratic function $\sim 1.4-0.53\mu^2$ (Fig. 3). This rather simple dependence may be related to the universality class on this line.

$P_B(w)$ is estimated to be zero at the origin. The inset of Fig. 2 shows $P_B(w)$ near the origin, indicating a power law. To characterize this behavior, we make an ansatz of

$$P_B(w) \sim w^\alpha \text{ as } w\to 0 \tag{18}$$

where $\alpha>0$. The optimized values of $\alpha(\mu)$ are shown in Table I. One sees that the $\alpha(\mu)$'s are stable, suggesting that $\alpha(\mu)$ is independent of μ at the incommensurate limit.

These numerical results suggest that the overall distribution is given by a generalized semi-Poisson form

$$P_B(w) = Aw^\alpha e^{-\beta w} \tag{19}$$

where A is a normalization constant. The exact semi-Poisson form, i.e., $\alpha=1$, $\beta=2$, has been reported at $(\lambda,\mu)=(2.0,0.0)$ [20]. Actually the normalization conditions allow only one parameter α with $\beta=\alpha+1$ and $A=(\alpha+1)^{\alpha+1}/\Gamma(\alpha+1)$. It is clear that such relations are not consistent with our results as shown in Table I. Especially the semi-Poisson statistics with $\alpha=1$ do not reproduce the index of the power-law behavior around the origin at $\mu=0$. Using a one-parameter fit by Eq. (19), we get $\alpha\sim 0.7$ for the overall distribution, which is much smaller than that estimated by Eq. (18). For $\mu\neq 0$, we get similar deviations. Thus we may conclude that the semi-Poisson form for $P_B(w)$ is only an approximation to the overall distribution.

TABLE I. The optimized indices on the critical line $\lambda=2$ and in the critical region. For the definitions of α,β, and δ, see Eqs. (17), (18), and (22), respectively. Also the value of α in the critical region is defined as $-\alpha'$.

λ	μ	α	β	δ
2.0	0.0	2.5(±0.1)	1.39(±0.07)	1.5(±0.2)
2.0	0.1	2.5(±0.1)	1.41(±0.07)	1.5(±0.2)
2.0	0.2	2.5(±0.1)	1.39(±0.06)	1.5(±0.2)
2.0	0.3	2.51(±0.08)	1.34(±0.05)	1.5(±0.1)
2.0	0.4	2.51(±0.08)	1.35(±0.05)	1.5(±0.2)
2.0	0.5	2.50(±0.06)	1.26(±0.04)	1.5(±0.2)
2.0	0.6	2.52(±0.07)	1.26(±0.04)	1.5(±0.2)
2.0	0.7	2.54(±0.07)	1.12(±0.07)	1.5(±0.2)
2.0	0.8	2.52(±0.07)	1.05(±0.08)	1.5(±0.1)
2.0	0.9	2.48(±0.04)	0.98(±0.11)	1.47(±0.04)
2.0	1.0			1.2(±0.3)
2.0	2.0	−1.46(±0.06)		1.34(±0.07)
2.0	4.0	−1.5(±0.1)		1.1(±0.1)
2.0	6.0	−1.37(±0.08)		1.3(±0.2)

C. Bandwidth distribution on $\mu=1$ and $\mu=\lambda/2$

Next, we investigate $P_B(w)$ on the other critical lines. It turns out that the behaviors are different from those on the critical line $\lambda=2$. Figure 4 shows $P_B(w)$ at $(\lambda,\mu)=(1.0,1.0)$. The large w behaviors do not show an exponential decay, but a milder one. Thus we make a generalized ansatz of

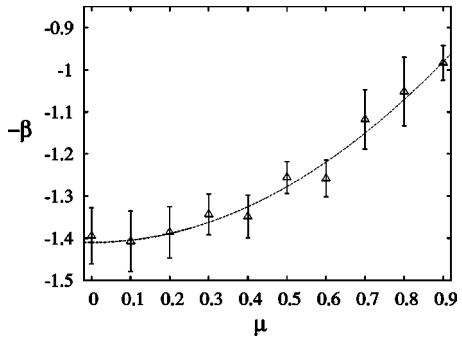

FIG. 3. μ dependence of index β along the critical line $\lambda=2$ for $q=514\,229$.

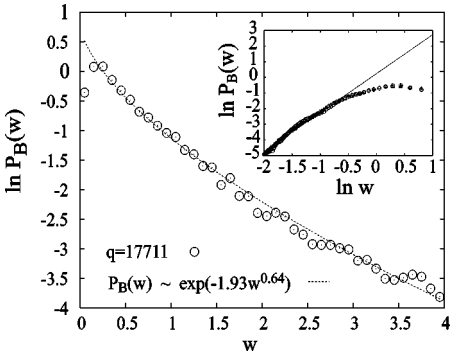

FIG. 4. The bandwidth distribution at $(\lambda,\mu)=(1.0,1.0)$, and the one near the origin (inset) for $q=17\,711$.

$$P_B(w) \sim e^{-\beta\omega^\gamma} \text{ as } w \to \infty \tag{20}$$

with $0<\gamma<1$. The optimized curve agrees well with the obtained data (Fig. 4). The behavior near the origin is also found to follow a power law (inset of Fig. 4). On the line $\mu=1$, the index α seems to be constant around 1.5. We find that the numerical data on the critical line $\lambda=2\mu$ can be also described by each ansatz (18) and (20). The index α is stable around 1.5 as in Table II, which is near the values on the critical line $\mu=1$.

The overall distribution on the critical lines $\mu=1$ and $\lambda=2\mu$ except for the bicritical point may be cast in the form

$$P_B(w) = Aw^\alpha e^{-\beta\omega^\gamma}. \tag{21}$$

This form of distribution was suggested in Ref. [8] for the level spacing distribution of disordered systems at the MI transition. The normalization conditions constrain

$$\beta = \left(\frac{\Gamma\left(\frac{\alpha+2}{\gamma}\right)}{\Gamma\left(\frac{\alpha+1}{\gamma}\right)} \right)^\gamma \text{ and } A = \frac{\gamma\beta^{(\alpha+1)/\gamma}}{\Gamma\left(\frac{\alpha+1}{\gamma}\right)}.$$

Our analysis does not support these constraints. Again, we tried a one-parameter fit varying $\alpha(\gamma)$ in Eq. (21) with the observed value of $\gamma(\alpha)$ fixed. We got values much smaller (larger) than the observed indices α (γ) around the origin (in the tail) for all the points we studied on the critical lines $\mu=1$ and $\lambda=2\mu$.

D. Bicritical point

We also investigate the bicritical point at $(\lambda,\mu)=(2.0,1.0)$. We show the results in Fig. 5 at $q=4181$. The convergence of the obtained distribution is slow, and we have not got information about the incommensurate limit.

E. Bandwidth distribution in the critical region

The values of α and γ on the critical lines $\mu=1$ and $\lambda=2\mu$ are considerably smaller than those on $\lambda=2$ ($\gamma=1$ there). This smallness of α and γ indicates the tendency of $P_B(w)$ on these critical lines to broaden both to the origin and the tail compared to $P_B(w)$ on $\lambda=2$. This may imply that the transport property becomes different when μ gets sufficiently large. To supplement this observation, we investigate the bandwidth distribution in the critical region [the region III in Fig. 1(b)]. $P_B(w)$ follows an inverse power law $P_B(w) \sim w^{-\alpha'}(\alpha'>0)$ there (Fig. 6). The values of α' are summarized in Table I. This behavior sharply contrasts with the one seen on the critical lines. The divergence of $P_B(w)$ at the origin implies the dominance of relatively flat bands, indicating that in most of the bands the wave function is close to being localized. Also, the power-law decay in the tail means the appearance of bands whose wave function is close to being extended.

F. Gap distribution

We also investigate the gap distribution $P_G(s)$. The gap distribution at $(\lambda,\mu)=(2.0,0.0)$ is known to follow an inverse power law [24,25], which diverges at the origin,

$$P_G(s) \sim s^{-\delta} \tag{22}$$

with $\delta\sim 1.5$. We find $P_G(s)$ along the three critical lines and in the critical region it also follows an inverse power law (inset of Fig. 6). The values of δ are shown in Tables I and II.

IV. DISCUSSION

From the two-dimensional point of view, the next-nearest-neighbor hopping term (μ-dependent term) is dominant in Eq. (9) in the critical region. Since y translation is canonically conjugate to x translation in a uniform magnetic field, the extension (localization) of the wave function in the y direction must be balanced by the localization (extension) in the x direction to satisfy the uncertainty principle. When μ is small, the x dependence of the wave function is determined by λ, the anisotropic parameter for the y direction. On the other hand, when μ is sufficiently large, as μ acts on the x and y directions equally, the wave function is sensitive to μ in both its x and y dependences. This makes the MI transition in the critical region different from that on the critical line

TABLE II. The optimized indices for the bandwidth distribution and level spacing distribution on the critical lines of $\mu=1$ and $\lambda=2\mu$. For the definition of γ, see Eq. (20).

λ	μ	α	γ	δ
0.5	1.0	1.55(±0.14)	0.41(±0.04)	1.29(±0.08)
0.75	1.0	1.48(±0.17)	0.52(±0.08)	1.3(±0.2)
1.0	1.0	1.48(±0.12)	0.65(±0.07)	1.3(±0.2)
1.25	1.0	1.61(±0.17)	0.53(±0.05)	1.4(±0.2)
1.5	1.0	1.48(±0.13)	0.60(±0.07)	1.29(±0.10)
2.5	1.25	1.44(±0.10)	0.54(±0.06)	1.31(±0.10)
3.0	1.5	1.61(±0.13)	0.51(±0.04)	1.3(±0.2)
3.5	1.75	1.49(±0.14)	0.38(±0.04)	1.5(±0.2)
4.0	2.0	1.43(±0.13)	0.60(±0.06)	1.3(±0.2)
4.5	2.25	1.64(±0.15)	0.64(±0.03)	1.3(±0.3)
5.0	2.5	1.34(±0.19)	0.50(±0.04)	1.4(±0.2)

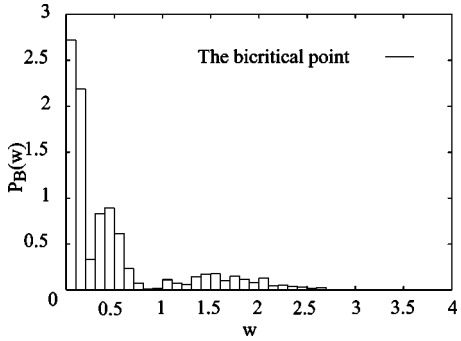

FIG. 5. The bandwidth distribution at $(\lambda,\mu)=(2.0,1.0)$ with $q=4181$.

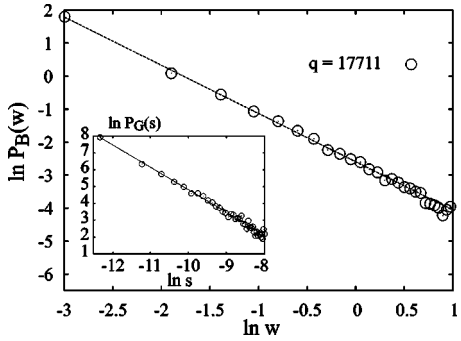

FIG. 6. The bandwidth distribution and level spacing distribution (inset) at $(\lambda,\mu)=(2.0,2.0)$ for $q=17\,711$.

$\lambda=2$, resulting in the increase of the bands close to being localized as well as the bands close to being extended. Thus the appearance of the inverse power law in the critical region and the differences of α and γ among the critical lines are consequences of the quantum nature of the system.

V. SUMMARY

We have seen that a systematic characterization by level statistics for a quasiperiodic system is possible. We have investigated the bandwidth $P_B(w)$ and gap distributions $P_G(s)$ for one-dimensional quasiperiodic Schrödinger equations at the MI transition and confirmed their variety as expected. We did not find that the bandwidth at the critical state is distributed according to the semi-Poisson distribution. We found a power law $P_B(w)\sim w^{\alpha}$ near the origin and a generalized exponential decay $P_B(w)\sim e^{-\beta w^{\gamma}}$ $(\alpha,\beta,\gamma>0)$ on the critical lines, while in the critical region $P_B(w)$ follows an inverse power law $\sim w^{-\alpha'}$ $(\alpha'>0)$. We gave an explanation for this variety of $P_B(w)$ by the quantum nature of the system. The surmise of a form $P_B(w)=Aw^{\alpha}e^{-\beta w^{\gamma}}$ gives only an approximation. The gap distribution $P_G(s)$ shows an inverse power law $\sim s^{-\delta}$ for the whole phase diagram. For the bicritical point, we did not get a conclusive result.

ACKNOWLEDGMENTS

Y.T. and K.I. thank S. Hikami for useful discussions. K.I. thanks A. Garcia-Garcia for discussion and M. Kohmoto for explaining previous results. K.I. has benefited from the Grand-in-Aid for Science (B), No. 1430114, of JSPS.

[1] See, for example, T. Guhr, A. Müller-Groeling, and H. A. Weidenmüller, Phys. Rep. **299**, 189 (1998).
[2] O. Bohigas, in *Chaos and Quantum Physics*, Proceedings of the Les Houches Summer School, edited by M. J. Giannoni, A. Voros, and J. Zinn-Justin (Elsevier, New York, 1991).
[3] J. Verbaarschot, Nucl. Phys. B (Proc. Suppl.) **53**, 88 (1997).
[4] E. P. Wigner, Proc. Cambridge Philos. Soc. **47**, 790 (1951).
[5] F. J. Dyson, J. Math. Phys. **3**, 140 (1962); **3**, 157 (1962); **3**, 166 (1962).
[6] B. L. Altshuler, I. Kh. Zharekeshev, S. A. Kotochigova, and B. I. Shklovskii, Sov. Phys. JETP **67**, 625 (1988).
[7] B. I. Shklovskii, B. Shapiro, B. R. Sears, P. Lambrianides, and H. B. Shore, Phys. Rev. B **47**, 11 487 (1993).
[8] A. G. Aronov, V. E. Kravtsov, and I. V. Lerner, JETP Lett. **59**, 39 (1994); Phys. Rev. Lett. **74**, 1174 (1995).
[9] I. Kh. Zharekeshev and B. Kramer, Jpn. J. Appl. Phys., Part 1 **34**, 4361 (1995); Phys. Rev. Lett. **79**, 717 (1997).
[10] M. Batsch, L. Schweitzer, I. Kh. Zharekeshev, and B. Kramer, Phys. Rev. Lett. **77**, 1552 (1996).
[11] L. Schweitzer and I. Kh. Zharekeshev, J. Phys.: Condens. Matter **7**, L377 (1995).
[12] T. Kawarabayashi, T. Ohtsuki, K. Slevin, and Y. Ono, Phys. Rev. Lett. **77**, 3593 (1996).
[13] E. Cuevas, Phys. Rev. Lett. **83**, 140 (1999).
[14] H. Hiramoto and M. Kohmoto, Int. J. Mod. Phys. B **6**, 281 (1992).
[15] M. Ya. Azbel, Zh. Eksp. Teor. Fiz. **46**, 929 (1964).
[16] D. R. Hofstadter, Phys. Rev. B **14**, 2239 (1976).
[17] S. Aubry and G. André, Ann. Isr. Phys. Soc. **3**, 133 (1980).
[18] C. Albrecht, J. H. Smet, K. von Klitzing, D. Weiss, V. Umansky, and H. Schweizer, Phys. Rev. Lett. **86**, 147 (2001).
[19] A. P. Megann and T. Ziman, J. Phys. A **20**, L1257 (1987).
[20] N. Evangelou and J.-L. Pichard, Phys. Rev. Lett. **84**, 1643 (2000).
[21] J. H. Han, D. J. Thouless, H. Hiramoto, and M. Kohmoto, Phys. Rev. B **50**, 11 365 (1994).
[22] D. J. Thouless, Phys. Rev. B **28**, 4272 (1983); Commun. Math. Phys. **127**, 187 (1990).
[23] P. G. Harper Proc. Phys. Soc., London, Sect. A **68**, 874 (1955).
[24] K. Machida and M. Fujita, Phys. Rev. B **34**, 7367 (1986).
[25] T. Geisel, R. Ketzmerick, and G. Petschel, Phys. Rev. Lett. **66**, 1651 (1991).